Received: 28 April 2018 | Revised: 4 July 2018 | Accepted: 9 July 2018

DOI: 10.1111/cns.13039

ORIGINAL ARTICLE

WILEY CNS Neuroscience & Therapeutics

Spontaneous activities in baroreflex afferent pathway contribute dominant role in parasympathetic neurocontrol of blood pressure regulation

Wen-Xiao Xu[1] | Jin-Ling Yu[2] | Yan Feng[2] | Qiu-Xin Yan[2] | Xin-Yu Li[2] | Ying Li[2] | Zhuo Liu[2,3] | Di Wang[2,3] | Xun Sun[2] | Ke-Xin Li[2] | Lu-Qi Wang[2,4] | Guo-Fen Qiao[2] | Bai-Yan Li[2]

[1]Department of Orthopedic Surgery, the 2nd Affiliated Hospital of Harbin Medical University, Harbin, China

[2]Department of Pharmacology (State-Province Key Laboratories of Biomedicine-Pharmaceutics of China, Key Laboratory of Cardiovascular Medicine Research, Ministry of Education), College of Pharmacy, Harbin Medical University, Harbin, China

[3]Herman B. Wells Center for Pediatric Research, Department of Pediatrics, Indiana University School of Medicine, Indianapolis, Indiana

[4]Department of Biomedical Engineering, Indiana University Purdue University Indianapolis School of Engineering and Technology, Indianapolis, Indiana

Correspondence: Bai-Yan Li and Guo-Fen Qiao, Department of Pharmacology, Harbin Medical University, #157 Bao-Jian Road, Harbin 150081, China (liby@ems.hrbmu.edu.cn; Qiaogf88@163.com).

Funding information
This work was fully supported by the research grants from the National Science Foundation of China (81573431 and 81773731), and and this project was also supported by Heilongjiang Postdoctoral Foundation.

Abstract

Aim: To study the dominant role of parasympathetic inputs at cellular level of baroreflex afferent pathway and underlying mechanism in neurocontrol of blood pressure regulation.

Methods: Whole-cell patch-clamp and animal study were conducted.

Results: For the first time, we demonstrated the spontaneous activities from resting membrane potential in myelinated A- and Ah-type baroreceptor neurons (BRNs, the 1st-order), but not in unmyelinated C-types, using vagus-nodose slice of adult female rats. These data were further supported by the notion that the spontaneous synaptic currents could only be seen in the pharmacologically and electrophysiologically defined myelinated A- and Ah-type baroreceptive neurons (the 2nd-order) of NTS using brainstem slice of adult female rats. The greater frequency and the larger amplitude of the spontaneous excitatory postsynaptic currents (EPSCs) compared with the inhibitory postsynaptic currents (IPSCs) were only observed in Ah-types. The ratio of EPSCs:IPSCs was estimated at 3:1 and higher. These results confirmed that the afferent-specific spontaneous activities were generated from baroreflex afferent pathway in female-specific subpopulation of myelinated Ah-type BRNs in nodose and baroreceptive neurons in NTS, which provided a novel insight into the dominant role of sex-specific baroreflex-evoked parasympathetic drives in retaining a stable and lower blood pressure status in healthy subjects, particularly in females.

Conclusion: The data from current investigations establish a new concept for the role of Ah-type baroreceptor/baroreceptive neurons in controlling blood pressure stability and provide a new pathway for pharmacological intervention for hypertension and cardiovascular diseases.

KEYWORDS

baroreflex afferent pathway, parasympathetic activity, sexual dimorphism, spontaneous activity

The first two authors contributed equally to this work

1 | INTRODUCTION

It has been widely accepted that the parasympathetic nerve activity plays a leading role against sympathoexcitation in the neurocontrol of circulation and stabilization of blood pressure.[1] Despite the close association of the baroreflex function with parasympathetic activation[2–4] and having the extensive studies on baroreflex at both afferent and efferent pathways,[5] the underlying mechanism at cellular and physiological level is still largely unknown due to the difficulties in handling these tissues for proper physiological measurements. Over the years, we have developed a highly reliable approaches for electrophysiological recording using vagus-nodose slice, which allows us demonstrating a critical female-specific Ah-type neurons in the nodose and their potential role in neurocontrol of blood pressure.[6–16]

It is well documented that the blood pressure is lower in females than that in age-matched males.[17] This notion is consistent with the recent observations reported in rodent models,[4,10,18] indicating that females have a much higher parasympathetic activity than males[19–24] and neuroprotective action of estrogen.[25] Our previous observation has shown that, in adult female rats, there is a female-specific subpopulation of myelinated Ah-type baroreceptor neurons (BRNs) in nodose[6,26] and baroreceptive neurons in tractus nucleus of solitary (NTS),[16,27] with which an important neuroanatomical structure supports for a critical parasympathetic activity in baroreflex afferent function in females. Based on electrophysiological properties, a low firing threshold and high excitability strongly suggest that Ah-type BRNs could be activated at a relatively lower blood pressure[2] due presumably to higher levels of expression of KCa1.1,[9,16] voltage-dependent Na^{+}[13,28] and HCN1[14,29] channels, which would make this neuron type a key player in parasympathetic activation. However, assumptive spontaneous discharge activities generated from this neuron group have never been reported so far, which is a non-negligible factor in maintaining constant parasympathetic outflow through baroreflex afferent pathway despite this activity has been shown successfully in somatic sensory system/dorsal root ganglia.[30] To this end, we launched our efforts to test the potential existence of these critical spontaneous activities in the first-order BRNs in the nodose and spontaneous synaptic currents in the second-order baroreceptive neurons in the NTS with afferent fiber type using vagus-nodose slices[8] and brainstem slices.[16] Here, we are able to successfully record the spontaneous activities in the second-order BRNs and second-order baroreceptive neurons, respectively, and provide our first-handed evidences to support the critical physiological function of Ah-BRNs in this unique sex-dependent baroreflex afferent pathway.

2 | METHODS

2.1 | Animals

All protocols about animals used in experiments were preapproved by Institutional Animal Care and Use Committee of Harbin Medical University, which are in accordance with the recommendations of the Panel on Euthanasia of the American Veterinary Medical Association and the National Institutes of Health publication "*Guide for the Care and Use of Laboratory Animals*" (https://www.nap.edu/readingroom/books/labrats/). Age-matched Adult male, ovaries intact (OVI) female and ovariectomized (OVX) female Sprague-Dawley (SD) rats (12-14 weeks weighing 220-250 g) were used in this study for nodose or brainstem slices preparations, as well as a long-term blood pressure and baroreceptor sensitivity measurements in vivo. Rats were directly purchased from Wei Tong Li Hua Experimental Animal Technology Co, Ltd, Beijing, China, with SPF grade and licensed under SCXK (Beijing) 2012-0001. All rats were maintained at the animal facility of School of Pharmacy, Harbin Medical University with a 12/12-hour light cycle for 3 days before they were used for experiments.

2.2 | Chemicals

Capsaicin (Cap, a TRPV1 agonist) was purchased from Sigma (St Louis, MO, USA); cyclothiazide (CTZ, a modulator of AMPA receptor for removing rapid desensitization at postsynaptic terminals), 2,3-Dihydroxy- 6-nitro-7-sulfamoyl-benzo(F) quinoxaline (NBQX, antagonist for non-NMDA), and iberiotoxin (IbTX, a selective blocker for a large conductance of Ca^{2+}- activated-K^{+} channel, KCa1.1) were purchased from Sigma; stock solutions were stored at −20°C and diluted using the bath solution right before experiments. During the experiment, drugs or toxins were applied through bath perfusion or micro-perfusion right on the patched neuron at flow rate no more than 1.0 mL/min.

2.3 | Vagus-nodose slice preparation

Adult female Sprague-Dawley rats were used for the preparation of nodose ganglion slices to study myelinated A- and Ah-type neurons as well as unmyelinated C-type nodose neurons.[7] The bilateral dissection of the vagal ganglia each with ~ 2.0 cm of their vagus nerve attached, ganglia slicing, and enzymatic digestion have been described elsewhere. Briefly, after dissection and digestion, the slices were then transferred to a Petri dish filled with 5.0 mL of Earls Balanced Salt Solution (Sigma) containing 1.0 mg/mL of type-II collagenase (Worthington Biochemical, Lakewood, NJ, USA) and incubated at 37°C for 45 min followed by fresh support medium with 5.0 mg/mL trypsin (Worthington Biochemical) at 37°C for an additional 25 minutes. The enzyme solution was then repeatedly replaced with chilled (~4°C) recording solution prior to transferring to the recording chamber.

2.4 | Horizontal brainstem slice preparation

Horizontal brainstem slices of the NTS region using adult male and age-matched female Sprague-Dawley rats were obtained following procedures described in details previously.[3,16,31] Briefly, slices were obtained from adult female and ovariectomized (OVX) female rats. Synaptic currents were evoked through stimulation from

a concentric bipolar electrode (FHC, Bowdoin, ME) placed on the solitary tract, approximately 1-3 mm from the medial NTS recording site. Synaptic characterization of NTS neurons was performed using five stimuli bursts of 200-μs duration delivered at 50 Hz, with a three second interval between each sweep. Stimulus intensity was gradually increased until excitatory postsynaptic currents (EPSCs) were repeatedly evoked.

Additionally, 50 nmol/L NBQX was applied to identify that this excitatory neurotransmission is mediated by rapid AMDA receptor activated by glutamate at the postsynaptic terminal, which is a crucial mechanism to ensure the effective neurotransmission under physiological condition.

2.5 | Aortic depressive nerve labeling

To verify the afferent modality of baroreceptor afferents, the aortic depressive nerve (ADN) was fluorescently labeled with DiI in a cohort of female rats (75-100 g) at least 4 weeks prior to electrophysiological experimentation to ensure having enough time for lipophilic dye to transport to NTS region.[11,32]

2.6 | Electrophysiological recording

Baroreceptor neurons in intact vagus-nodose slice and the location of NTS in the horizontal brainstem slices were determined as previously described.[10,11] Spontaneous and evoked discharges of AP were recorded using intact vagus-nodose slices.[6,15] The spontaneous synaptic currents were recorded using horizontal brainstem slice.[14,20] All electrophysiological experiments were conducted using a standard whole-cell patch-clamp technique.[7] Spontaneous synaptic current were also recorded on the second-order NTS-baroreceptive neurons using the standard whole-cell patch-clamp technique. After each test, 100 nmol/L of capsaicin (Cap, Sigma) was applied to further confirm the afferent fiber type of tested neurons.

2.7 | Recording solutions

For vagus-nodose slice recording, extracellular and intracellular solutions were exactly same as our previously described.[7,8]

To mimic the physiological Ca^{2+} in rat CSF and to prevent saturation of neurotransmitter release, experiments used 1 mM $[Ca^{2+}]_{o.}$[33,34] Low calcium (1 mmol/L) ACSF has the same composition as ACSF as used in previous studies, with the exception of 1 mmol/L $CaCl_2$ and 2 mmol/L $MgCl_2$ in place of 2 mmol/L $CaCl_2$.[3,31] Sensitivity to 100 nmol/L of the TRPV1 agonist capsaicin (Cap) enables us to reliably identify synapses associated with unmyelinated (C-type), or myelinated (A- and Ah-types) visceral afferents.

2.8 | Neurons identification

According to measured conduction velocity (CV) at cell-attached configuration using vagus-nodose slice,[7,15] those neurons showing fast CV > 10 m/s without the repolarization hump were classified as myelinated A-types, those showing faster CV > 4 m/s with repolarization hump were classified as myelinated Ah-types, while, those neurons showing slow CV < 1/s with significant repolarization hump at room temperature were classified as unmyelinated C-types.[7] The baroreflex modality of the first-order neurons were also verified by the fluorescence at cell body[11] with DiI transported along with the afferent fibers.

Only synapses that meet the following criteria were considered as the second-order NTS neurons and used for further study: jitter (SD of latency) ≤200 μs and the amplitude plateau of excitatory postsynaptic currents (EPSCs) with increases in stimulus intensity.[33,35] After a synapse is identified as the 2nd order, the stimulus intensity is fixed at a level 1.5-2.5X threshold throughout the experiment. The second-order baroreceptive neurons were identified via surrounding fluorescence that is boutons formed by the synapse raised from the first-order baroreceptor neurons.[3,9,16,31]

2.9 | Arterial Baroreflex sensitivity

The arterial was cannulated to connect the physiological pressure transducer (AD Instruments MLT 844, Norway), which was used for measuring the change of mean arterial blood pressure (MABP) and heart rate (HR) automatically at the same time. Phenylephrine (PE; Sigma Chemical) or sodium nitroprusside (SNP; Sigma Chemical) were injected by indwelling venous catheter to induce transient increase or decrease in BP with three different doses (2, 5, and 10 μg/kg) respectively.[36] The averaged ratio of HR and MABP (ΔHR/ΔMABP) was designed as the symbol of BRS, which is applied to each dose of PE and SNP. All the data processing was applied using the software of Labchart 7 (AD Instruments, Bella Vista, Australia).

2.10 | Surgical ovariectomy

The surgery was performed following protocols described in details previously.[37,38] Briefly, anesthetized animals (combination of xylazine 10 mg/kg and ketamine 75 mg/kg) were placed in a lateral position, and both flanks were shaved and cleaned using chlorhexidine scrub and disinfected with 70% ethanol and povidone iodine (7.5%). A 2.0-cm incision was made on the left lateral side along a line spanning from the 2nd to the 5th lumbar vertebra, using a scalpel blade. The left ovary and associated fat were located and externalized by gentle retraction. After removal of the bilateral ovaries, peritoneal cavity, muscle layers, and skin were closed successively with 4-0 absorbable sutures and then penicillin (80 000 Units) was given via intramuscular injection. Four weeks after ovariectomy, a part of them were administrated 17β-estradiol (17β-E2) via subcutaneous injection (10 μg/kg, once daily) delivered in 200 μL sesame oil[39] for another 3 weeks, which were sacrificed for experimental use.

2.11 | Data analyses

Clampfit (Molecular Devices; Sunnyvale, CA, USA) was used for initial data readings and excel for statistical analysis (Microsoft, Northampton, MA, USA). Trace filtering and data graphing were accomplished by origin (Microsoft). A paired or unpaired *t*-test and ANOVA were applied where appropriate. "n" is the numbers of completely recording from vagus-nodose slice and brainstem slice preparations. The averaged data were presented as mean ± SD. The *P* value of equal or less than 0.05 was considered statistically different.

3 | RESULTS

Our extensive studies performed using either isolated nodose neurons or nodose slice preparations have showed that myelinated A- and unmyelinated C-type baroreceptor neurons (BRNs) were observed in both adult male and female rats with no significant difference in electrophysiological characters,[6,8] so, to simplify the test, the adult female rats were used to prepare the vagus-nodose slices and brainstem slices. To the concern of the effect of estrus cycle of adult female rats on the recordings, the control study was also conducted as the routine with OVX rats.

3.1 | Evoked action potential (AP) in baroreceptor neurons (BRNs) of nodose

On vagus-nodose slices,[7] electrophysiological analyses were performed on evoked AP to establish a proper condition for later recordings of spontaneous activities. A giga- seal/cell-attached condition was reached in BRNs[10] with voltage-clamp protocol. The conduction velocities (CVs) at room temperature (22-23°C) were evaluated according to the responses evoked by vagal stimulation (indicated as dash dot line in Figure 1) as myelinated A- (averaged at 15.4 ± 3.17 m/s ranging from 12 ~ 16 m/s, n = 13), Ah- (averaged at 11.6 ± 7.89 m/s ranging from 5 ~ 21 m/s, n = 17), and unmyelinated C-type (averaged at 0.72 ± 0.21 m/s ranging from 0.3 ~ 0.8 m/s, n = 77) BRNs (Figure 1B-D), respectively, with a superthreshold stimulus intensity under cell-attached configuration.[6,8] Apparently, the repolarization humps as the waveform signature (indicated by arrowheads in Figure 1C,D) were clearly observed in both identified Ah- and C-type BRNs (Figure 1C,D). Although CVs in either A- or Ah-types were within the range of myelinated afferents, the repolarization humps was only seen in Ah-types. Collectively, these experimental procedures[7,8,15] allowed us to accurately identify the afferent fiber types in real-time right before current- or voltage-clamp recordings with proper intracellular and extracellular solutions.

3.2 | Spontaneous events of BRNs at cell-attached condition under voltage-clamp mode

Despite the spontaneous synaptic currents were demonstrated in the second-order NTS neurons,[3] the spontaneous activities generated from

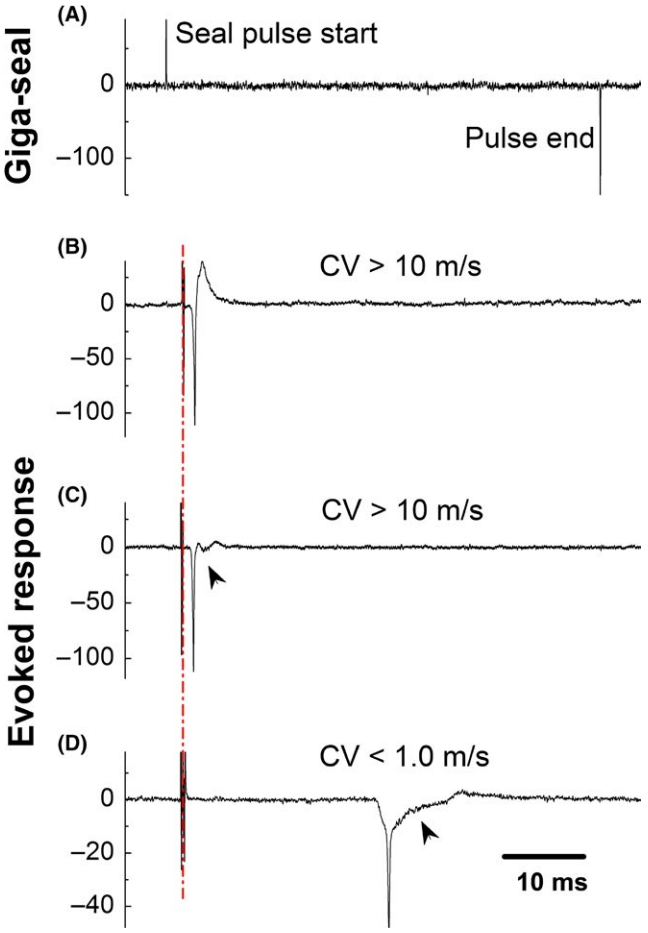

FIGURE 1 Identification of afferent fiber type based upon the conduction velocity conjugated with repolarization hump under the cell-attached condition. (A) A typical Giga- seal using the voltage-clamp protocol with 1 mV test pulse and 80-ms duration holding at −70 mV; (B-D) Evoked response and measured conduction velocity (CV) to identify myelinated A- (CV > 10 m/s with smooth repolarization), Ah- (CV > 10 m/s with clear repolarization hump indicated as arrow head), and unmyelinated C-type (CV < 1.0 m/s clear repolarization hump indicated as arrow head) baroreceptor neurons (BRNs) of nodose ganglion slice prepared using adult female rats, respectively; CV was evoked by vagal stimulation at room temperature under the current-clamp configuration before rupturing the cell membrane. Dash dot line represents the artifact of vagal stimulation. The horizontal scale bar in (D) also applied for (A-C)

visceral afferent neurons-nodose neurons (the first-order neurons) was not reported. By reviewing our recordings with nodose slice conjugated with aortic depressive nerve (ADN) labeling technique (n = 20 slice preparations),[11,32,35] interestingly, we were able to capture the spontaneous events generated from BRNs at cell-attached and voltage-clamp condition, rather than nonlabeled/general population of neurons of nodose. Considering the waveform signature (Figure 2, indicated by arrowheads) and CV, these spontaneous events were originated from myelinated A- (Figure 2A, n = 13) and Ah-type BRNs (Figure 2B,C, n = 17), but none of them were from unmyelinated C-types (data not shown). The percentages of myelinated A- (12.14%), Ah- (15.88%), and

unmyelinated C-type (71.96%) among the total population were consistent with the previous reports.[8,12] Notably, the spontaneous activities were only seen in recordings using tissue slices but not the isolated neurons of nodose, suggesting that the recording using vagus-nodose slice is more relevant to the physiological condition.

3.3 | Spontaneous events of BRNs at cell-attached condition under current-clamp mode

We were also able to observe the spontaneous events at cell-attached condition when switching recording from voltage-clamp to current-clamp mode. These spontaneous events with higher frequency were confirmed in A-type (Figure 2E) BRNs (20 ± 9 Hz) compared with the lower frequency in Ah-types (Figure 2G) BRNs (12 ± 6 Hz, $P < 0.01$ vs A-type) without vagal stimulation. The afferent fiber-types were also verified by the waveform signatures (Figure 2E,G, insets) and CVs evoked by superthreshold vagal stimulation. Intriguingly, the spontaneous events were also seen in both A- and Ah-type BRNs with stimulus intensity below threshold (Figure 2F,H, insets indicated by black triangle), suggesting that these spontaneous events were not associated with the vagal stimulation, as they appeared either right before or far behind the stimulation. Even so, these spontaneous events (Figure 2) were significantly reduced in Ah-types after ovariectomy (data not shown) without changing the waveform signature, indicating that these spontaneous events are closely related to the excitability of this neurogroup.

3.4 | Spontaneous discharges of BRNs at whole-cell configuration

Although we were able to see the spontaneous activities under cell-attached mode (without rupturing cell membrane), we were curious of the status under the whole-cell current-clamp condition (with rupturing cell membrane). As expected, the spontaneous discharges generated from the resting membrane potential were clearly seen in both A- (Figure 3A,C) and Ah-type (Figure 3B,D) BRNs, but not in C-types and Ah-types of OVX (data not shown). The spontaneous discharges observed from both A- and Ah-types

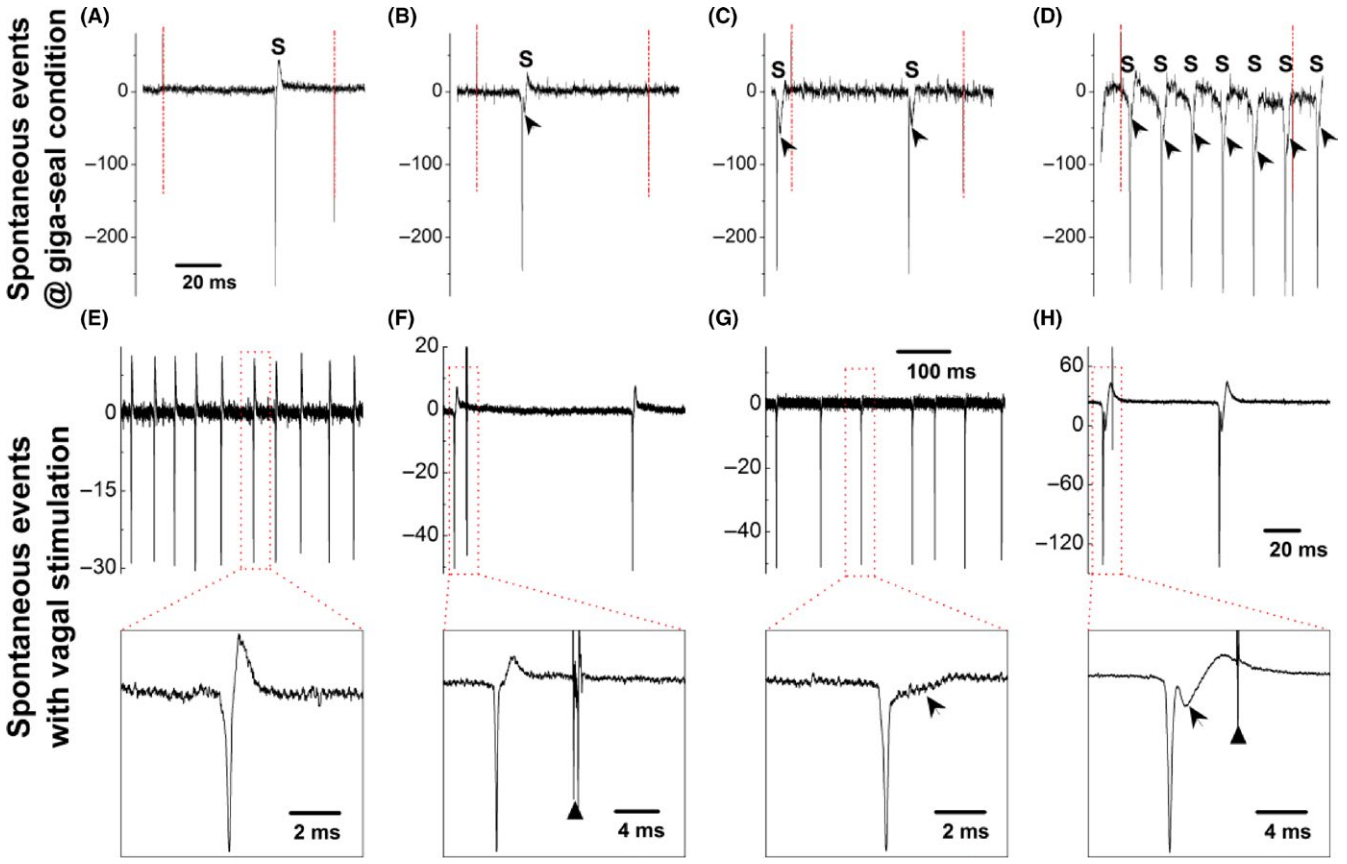

FIGURE 2 Spontaneous events (S) observed in myelinated A- (A) and Ah-type (B-D) baroreceptor neurons (BRNs) of nodose slice preparation using adult female rats under the giga-seal condition with voltage-clamp protocol before rupturing the cell membrane. Arrow heads represent the repolarization hump. The horizontal scale bar in (A) also applied for (A-C). Dash-dot line represents the seal pulse start and the end. Spontaneous events (S) recorded on myelinated A- (E) and Ah-type (G) baroreceptor neurons (BRNs) under the current-clamp mode without vagal stimulation and holding potential before rupturing the cell membrane; Spontaneous events (S) recorded on myelinated A- (F) and Ah-type (H) BRNs under the current-clamp mode with vagal stimulation (stimulus intensity below threshold) and without holding potential before the rupturing the cell membrane. Insets present the expended timescale to clearly demonstrate the repolarization hump (indicated as the arrowheads), black triangles present the time of vagal stimulation

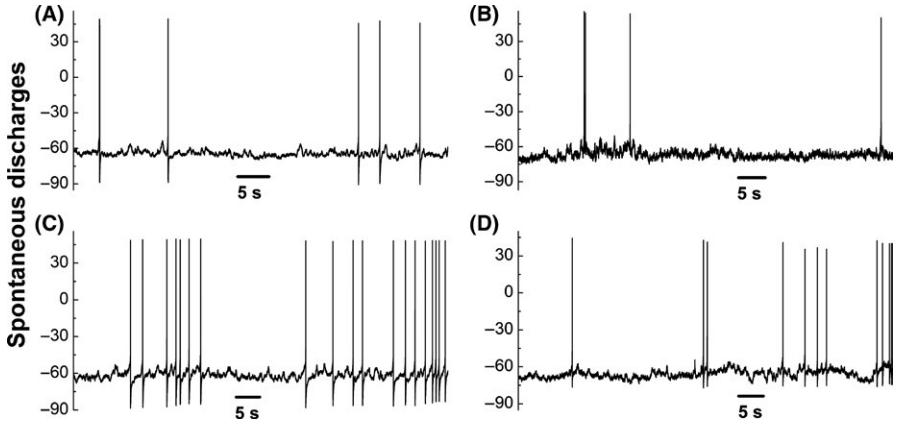

FIGURE 3 Spontaneous discharges of myelinated A- (A and C) and Ah-type (B and D) baroreceptor neurons (BRNs) nodose slice preparation of adult female rats from resting membrane potential (RMP) under the whole-cell current-clamp configuration

were irregular, likely suggesting the instantaneous change in BP fluctuation in vivo. The averaged frequency was overlapped between A- and Ah-types with slightly higher in A-types (9.21 ± 4.77 ranging from 3 to 16 spike/min) compared with Ah-types (7.47 ± 4.18 ranging from 2 to 10 spike/min, $P > 0.05$ vs A-type) at similar resting membrane potential. This result implies that myelinated BRNs are more critical to initiate parasympathetic drives through baroreflex. More importantly, due to its female-specific distribution,[6,12] the Ah-type BRNs are likely the key players in retaining relatively potent parasympathetic drives in females.[10]

3.5 | Spontaneous synaptic currents of baroreceptive neurons of nucleus tractus solitarius (NTS)

Previously, we have shown the spontaneous synaptic currents in NTS neurons of adult male rats.[3,31] Here we carried out similar experiments using brainstem slice of adult female rats. The afferent fiber type of baroreceptive neurons of NTS can be recognized by their different responses to Cap (100 nmol/L).[3,16] Myelinated A-type is a Cap-insensitive neurons without delay of excitation (Figure 4A); myelinated Ah-types are a similarly Cap-insensitive neurons that show a slightly delay of excitation (Figure 4B) and express a large conductance of Ca^{2+}-activated potassium channels (KCa1.1).[16] Unmyelinated C-type baroreceptive neurons are Cap-sensitive with significant delay of excitation (Figure 4C). Interestingly, the robust spontaneous synaptic currents were only observed in A- (Figure 4D) and Ah-type (Figure 4E) baroreceptive neurons of NTS, but not in C-types (Figure 4F), consistent well with the observation seen in BRNs in the nodose.

3.6 | The dynamics of excitatory postsynaptic currents and inhibitory postsynaptic currents in baroreceptive neurons of NTS

The spontaneous synaptic currents contain excitatory (EPSCs) and inhibitory postsynaptic currents (IPSCs). The outcome of baroreflex function is dependent upon which of these two dominates the spontaneous activity. The dynamic changes in rise time, decay time, and mean amplitude are significantly differ between EPSCs and IPSCs, which can be used as electrophysiological signature to define them.[3]Based on these signatures, we analyzed the dynamic properties of all tested myelinated A- (Figure 5A), Ah- (Figure $5_{1\text{-}3}$) and unmyelinated C-type (Figure 5B) baroreceptive neurons of NTS (Table 1), which include the dynamic changes in rise and decay time. Apparently, even though the rise and decay time differed between EPSCs and IPSCs in each categorized neuron, the significant difference of these two parameters was not reached among all 3 categories. However, the afferent-specific difference of mean amplitude of EPSCs in Ah- and C-types, but not in A-type baroreceptive neurons, was significantly higher (more than doubled) than that of IPSCs, suggesting that the excitatory neurotransmitter-glutamate released from its terminals is dominant in baroreflex. To evaluate if the dynamic changes the rise time, decay time, and the amplitude of EPSCs and IPSCs, the similar observations were also conducted using OVX female rats and the results showed that those parameters of EPSCs and IPSCs significantly changed to the levels of unmyelinated C-type like (data not shown).

3.7 | Afferent-specific high frequency of spontaneous EPSCs in myelinated Ah-type baroreceptive neurons of NTS

As we shown above, the mean amplitude of EPSCs in Ah-types is significantly larger than that of IPSCs. However, the more meaningful impact for the potent sympathoinhibition is dependent upon the frequency of the dominant afferent-specific events of spontaneous EPSCs. We therefore analyzed the ratio of EPSCs and IPSCs frequencies in each category of baroreceptive neurons in NTS. Remarkably, the frequency of spontaneous EPSCs (Figure 5D, at least 69 events as indicated with black triangle) was significantly higher than that of IPSCs (Figure 5D, maximal 22 events as indicated with black filled circle) recorded in the same Ah-type baroreceptive neurons. The averaged events per recording (five traces from $T_{1\text{-}5}$) was 64.8 ± 18.4 and 20.3 ± 7.24 for EPSCs and IPSCs ($P < 0.01$, n = 6 recordings),

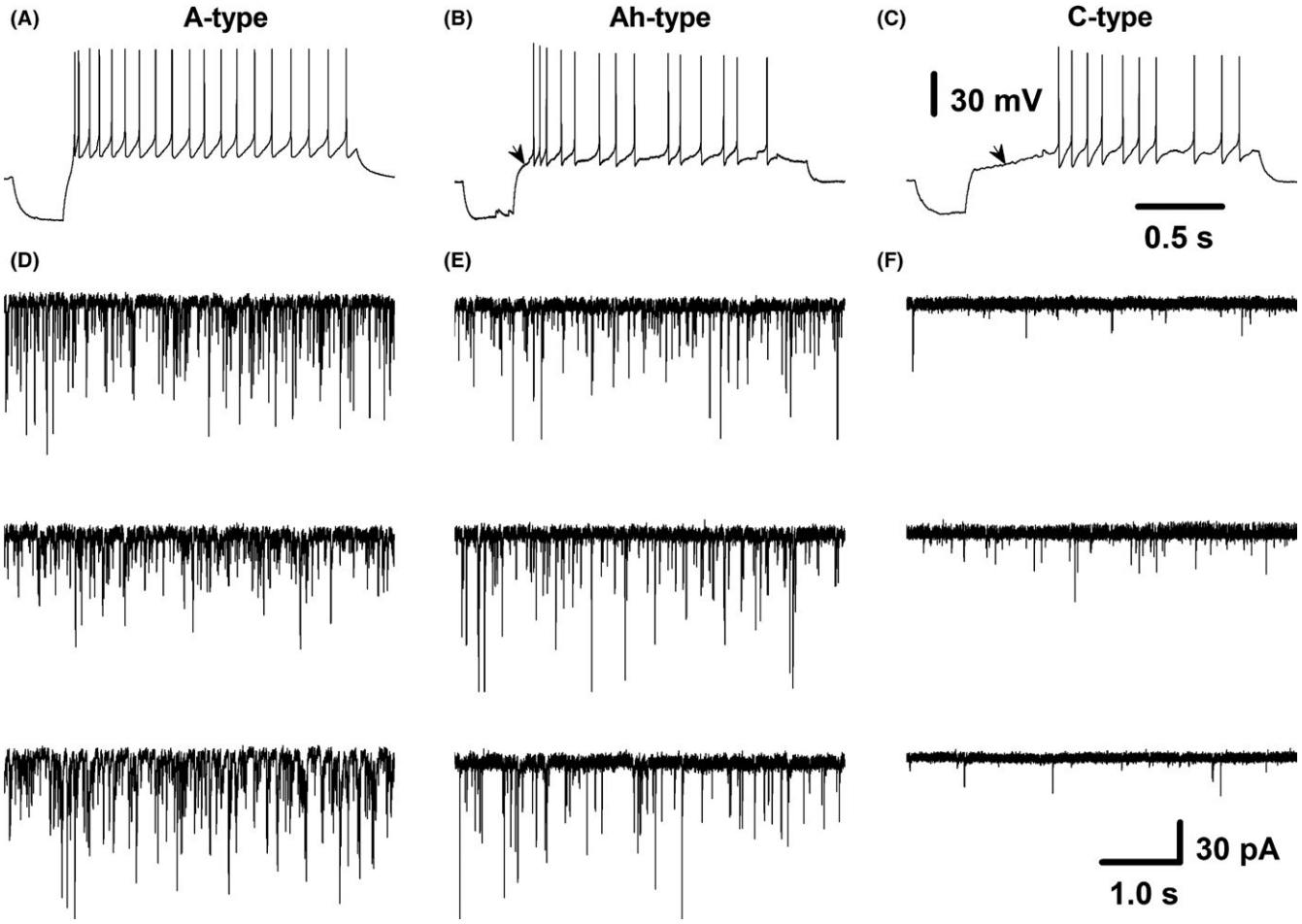

FIGURE 4 Spontaneous synaptic currents from identified myelinated A-, Ah- and unmyelinated C-type baroreceptive neurons of nucleus tractus solitarius (NTS). Baroreceptive modality was verified by the fluorescence around the neurons through aortic depressive nerve (ADN) labeling with DiI; baroreceptive fiber type was identified by capsaicin (Cap) and delay excitation; (A-C) representative recordings of myelinated A-type (Cap-insensitive, without delay excitation), myelinated Ah-type (Cap-insensitive, with slight delay excitation), and unmyelinated C-type (Cap-sensitive, with dramatic delay excitation), respectively; (D), three examples of spontaneous synaptic currents from A-type baroreceptive neurons; (E), three examples of spontaneous synaptic currents from Ah-type baroreceptive neurons; (F), three examples of spontaneous synaptic currents from C-type baroreceptive neurons. Scale bars in (C) also applied for (A) and (B); scale bars in (F) also applied for other spontaneous synaptic current recordings

respectively. The ratio of EPSCs:IPSCs was estimated at least 3:1. In stark contrast, the ratio of EPSCs:IPSCs was close to 1:1 in both myelinated A- (around 85 events for EPSCs and IPSCs, Figure 6A) and unmyelinated C-type (around 11 events for EPSCs and 10 events for IPSCs, Figure 6B) baroreceptive neurons of NTS. It is worth mentioning that the frequency of both of EPSCs and IPSCs obtained from Ah-types of intact female rats was markedly declined to the level of C-type baroreceptive neurons with the ratio of EPSCs/IPSCs close to 1:1 after the OVX procedure (data not shown).

3.8 | Dominant parasympathetic activity evaluated by blood pressure and baroreceptor sensitivity

Taken all electrophysiological data from this observation together, spontaneous discharge in female-specific distribution of myelinated Ah-type BRNs and baroreceptive neurons could initiate a strong parasympathetic drives to maintain relatively lower BP and higher baroreceptor sensitivity (BRS). In order to further confirm this hypothesis, BP and heart rate (HR) of adult male, age-matched female and ovariectomized (OVX) female rats were monitored for 6 consecutive weeks using tail-clamp procedure[10] and these data showed that BP and HR maintained consistent levels during the observation. Intriguingly, in intact females, the BP was lower and the HR was higher from the 2nd week ($P < 0.05$ or $P < 0.01$ *vs.* male; Figure 7A,B). The changes in BP and HR measured by tail-clamp technique were almost identical to those measured directly by the cannulation of femoral artery (data not shown). Apparently, both BP and HR observed in OVX rats were reached to the equivalent levels of those seen in males ($P > 0.05$ *vs.* male). Whether or not these differences in the BP and HR were dominated by the baroreflex afferent function, the BRS (ΔHR/ΔMABP, the mean arterial BP) [18] was also tested in the presence of phenylephrine (PE) or sodium nitroprusside (SNP) and the results indicated that the BRS in intact female was dramatically higher than those in male and OVX at all tested concentration of PE and SNP ($P < 0.05$; Figure 7C,D).

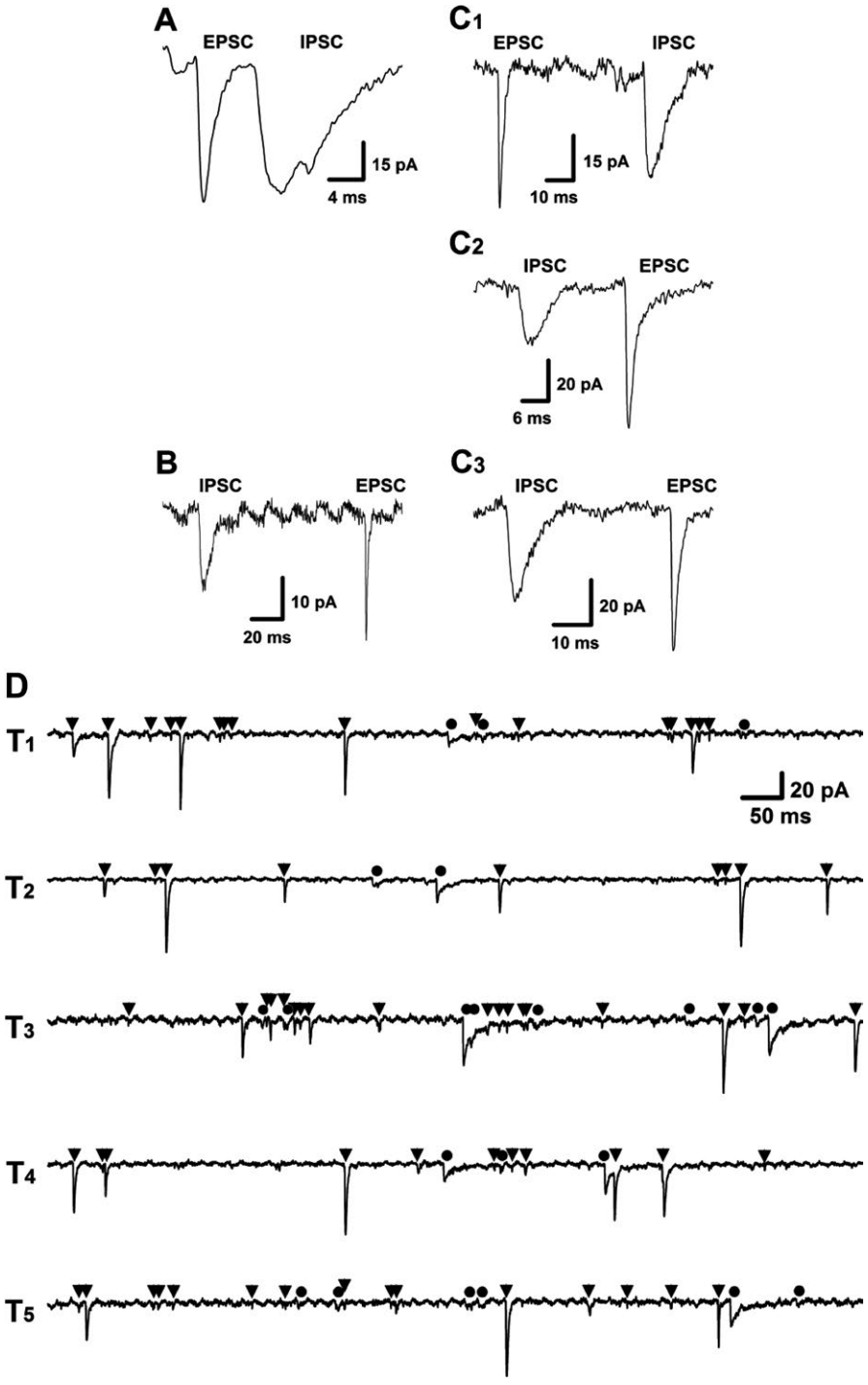

FIGURE 5 Representative traces of excitatory postsynaptic currents (EPSCs) and inhibitory post-synaptic currents (IPSCs) from identified myelinated A- (A), Ah- ($C_{1\text{-}3}$) and unmyelinated C-type (B) baroreceptive neurons of nucleus tractus solitarius (NTS). The dynamic changes in rise time, decay time, and mean amplitude were quantified in each tested afferent-specified neurons and the differences between EPSC and IPSC in each category neurons were described in Table 1. 20 μmol of NBQX and 100 μmol of Bicuculline were applied for selectively block the EPSCs and IPSCs, respectively. The representative recordings (D) of spontaneous synaptic currents from electrophysiologically and pharmacologically identified myelinated Ah-type baroreceptive neuron of NTS. EPSCs and IPSCs were indicated as ▼ and ●, respectively; $T_{1\text{-}5}$ presented as five consecutive episodes of recordings with 3-sec interval. The scale bar in T_1 also applies for T_2-T_5

These in vivo data were strongly supported by the notions that the dynamic parameters of EPSCs and IPSCs, as well as the ratio of EPSCs/IPSCs changed by lacking of estrogen.

4 | DISCUSSION

4.1 | The major finding

The derangement of sympathetic and parasympathetic cardiovascular regulation is one of the most widely accepted and tested hypotheses for cardiovascular diseases. An increased sympathetic nerve activity and a reduction in vagal cardiac tone are associated with and largely responsible for the appearance of the disease state high blood pressure.[40–42] The sympathetic hyperactivity is likely to be accompanied by an impaired vagal influence on the heart,[43] in which baroreflex mechanism is thought to be relatively more important in stabilizing blood pressure when compared to its other functions, such as the determination of the average levels of blood pressure.[44] The multiple lines of evidences have supported a causal role of autonomic dysfunction in hypertension, showing that

TABLE 1 The comparison of the properties of spontaneous synaptic currents of excitatory (EPSCs) and inhibitory postsynaptic currents (IPSCs) recorded from pharmacologically and electrophysiologically identified baroreceptive neurons of nucleus tractus solitarius (NTS) using adult female rats

	Rise time/ms		Decay time/ms		Mean amplitude/pA	
	EPSCs	IPSCs	EPSCs	IPSCs	EPSCs	IPSCs
A-type	1.24 ± 0.4	2.5 ± 0.7*	6.2 ± 4.2	36 ± 17**	57 ± 17	54 ± 15
Ah-type	1.27 ± 0.6	2.8 ± 0.5*	5.8 ± 3.9	39 ± 18**	54 ± 12§	22 ± 16**##§
C-type	1.28 ± 0.7	2.8 ± 0.9*	7.1 ± 5.1	42 ± 16**	23 ± 8	13 ± 6*

The rise time, decay time, and the mean amplitude of EPSCs and IPSCs were analyzed and compared between EPSCs and IPSCs, or each of them among the different groups of neurons. The averaged data were presented as mean ± SD.
*$P < 0.05$ and
**$P < 0.01$ vs EPSC;
##$P < 0.01$ vs A-types;
§$P < 0.05$ vs C-type, n = 5, 6, and 8 for A-, Ah-, and C-types.

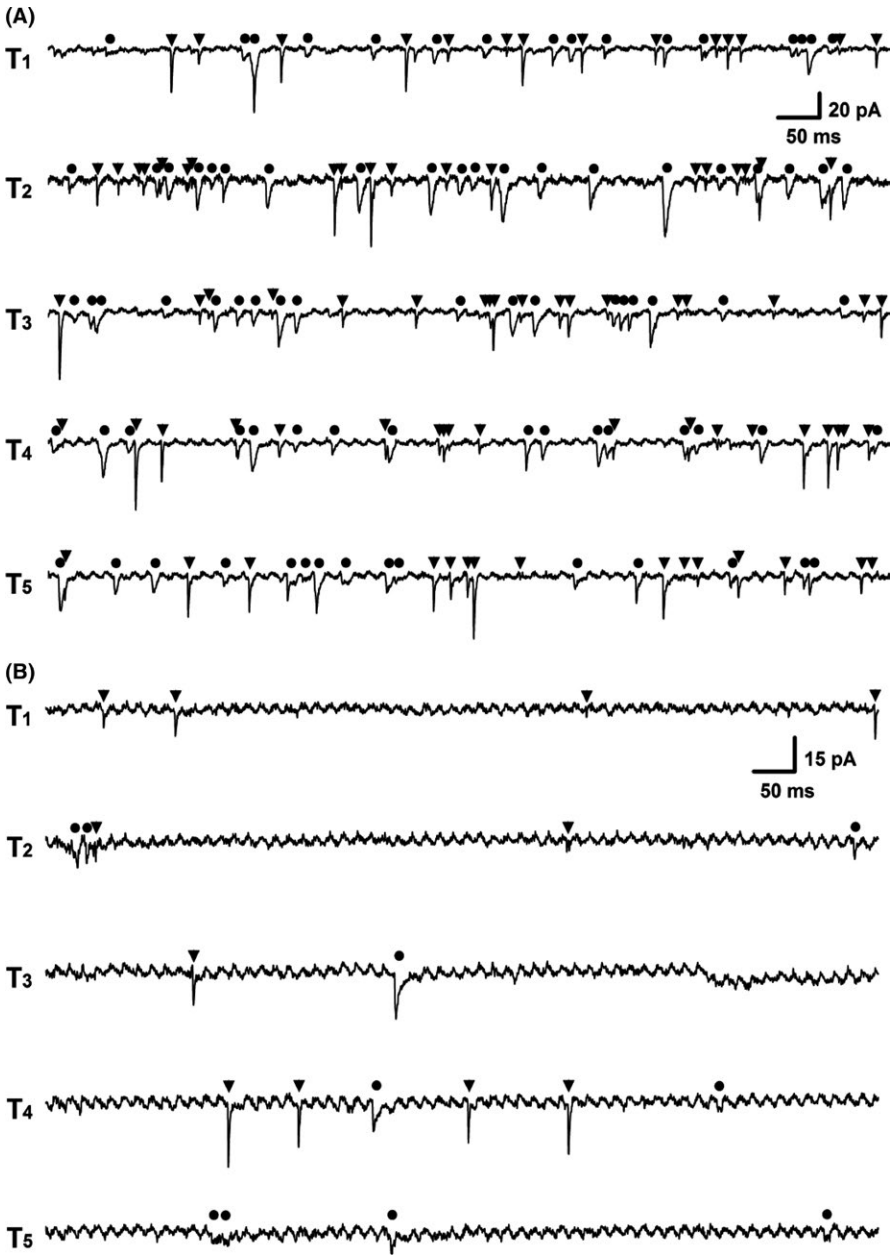

FIGURE 6 The representative recordings of spontaneous synaptic currents from electrophysiologically and pharmacologically identified myelinated A-type (A) and C-type (B) baroreceptive neuron of NTS. EPSCs and IPSCs were indicated as ▼ and ●, respectively; $T_{1\text{-}5}$ presented as 5 consecutive episodes of recordings with 3-s interval. The scale bar shown in T_1 also applied for $T_{2\text{-}5}$

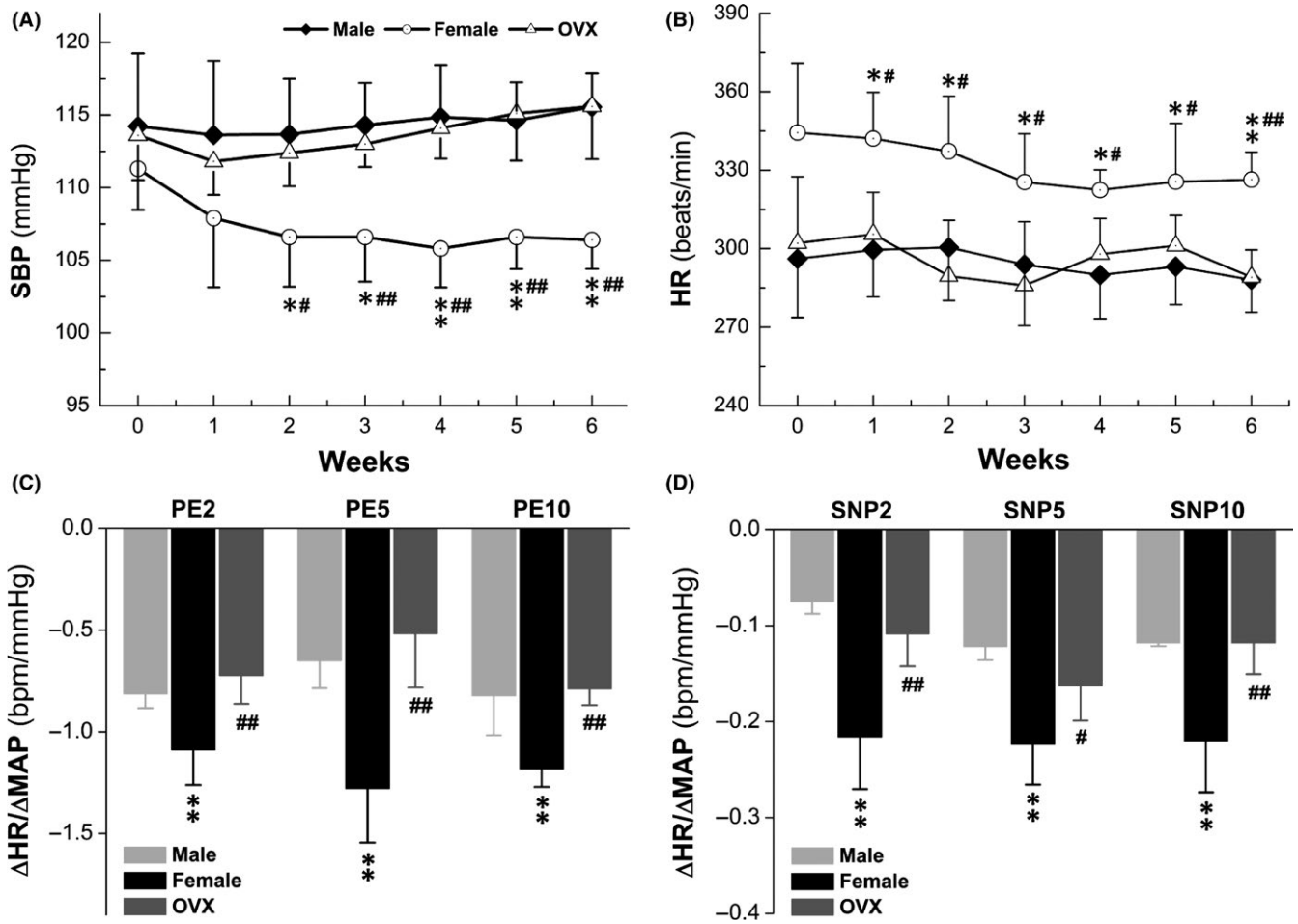

FIGURE 7 Changes in systolic blood pressure (SBP), heart rate (HR), and baroreceptor sensitivity (BRS) in adult male, age-matched female and ovariectomized (OVX) female rats. SBP and HR were collected from tail-clamp technique; phenylephrine (PE) and sodium nitroprusside (SNP) were applied through femoral artery catheterization; BRS was presented as by ΔHR/ΔMABP that were collected in the presence of 2, 5, and 10 μg/kg of PE or SNP (A and B): BP and HR measurements during 6 consecutive weeks; (C and D): BRS Changes during 6 wk. Averaged data were expressed by mean ± SD, n = 6 for male and OVX rats, n = 7 for female rats. $^{*}P < 0.05$ and $^{**}P < 0.05$ vs male, $^{\#}P < 0.05$ and $^{\#\#}P < 0.05$ vs OVX

hypertensive individuals and those in the early stages of hypertension have an increased sympathetic and a reduced cardiac vagal drive.[1,22,45] All above observations have clearly pointed out that the predominant role of parasympathetic tone for blood pressure regulation in healthy subjects.[46] However, the underlying mechanism by which the dominant role of parasympathetic activity in stabilizing blood pressure remains largely unknown.

This study provides three major direct evidences to support a higher parasympathetic activity in female rats. Firstly, the spontaneous discharge of APs has been confirmed in the female-specific subpopulation of Ah-type baroreceptor neurons as well A-types; secondly, a similar pattern of spontaneous synaptic currents has also been discovered in the female-specific subpopulation of Ah-types baroreceptive neurons of NTS; finally and the most importantly, a significantly higher frequency of EPSC events when compared to IPSC events has been only seen in Cap-insensitive Ah-type baroreceptive neurons in NTS, rather than A- and C-types. Taken all these major findings together, we have confirmed for the first time that the spontaneous discharge at the first-order Ah-type baroreceptor neurons triggers more glutamate release from its terminals. This finding is supported by the notion of the dominant EPSC events observed in the second-order Ah-type baroreceptive neurons of NTS. Moreover, these relayed events at baroreflex afferent pathway lead to an increased level of parasympathetic drives through the efferent loop of baroreflex, which helps to stabilize the blood pressure and maintain a relatively lower blood pressure in the normal females.

4.2 | Crucial role of female-specific distribution of myelinated Ah-type baroreceptor neuron in baroreflex afferent function and neurocontrol of circulation

In a series of recent studies, it has been shown that women exhibit higher parasympathetic activity during normal condition when compared to age-matched men. In addition, females have normally lower

systolic blood pressure but more variability of heart rate, a specific indication of a more dominant parasympathetic activity.[19–21,23,24] These findings in human are in line with previous studies in rodents showing lower systolic blood pressure due mainly to a more prominent baroreflex afferent function in adult female rats.[2,9,16,27] The obvious question has been why females demonstrate a higher parasympathetic activity when compared to males.[47,48] It can be explained partly by the female-specific distribution of myelinated Ah-type baroreceptor/baroreceptive neurons in both NG[6] and NTS[16] likely due to their relatively higher parasympathetic activity at cellular level.[2] However, it is not clear whether this mechanism is supported by the spontaneous discharge of baroreceptor neurons of NG and the spontaneous synaptic currents of NTS among myelinated A-, Ah, and unmyelinated C-type afferents. Our current study provides the first-handed evidences to support the hypothesis and have further defined the mechanism.

4.3 | Clinical relevance

Baroreflex is the fast and most efficient feed-back control of homeostasis in the neurocontrol of blood pressure. The sexual dimorphism in baroreflex afferent function has extensively been studied in our series of investigation, in which the female-specific distribution of myelinated Ah-type baroreceptor and baroreceptive neurons in nodose and NTS is the key player. The spontaneous activity of these Ah-neurons triggers the significant release of glutamate in their presynaptic terminal leading to the dominant parasympathetic efferents within the baroreflex in females. This result provides further solid evidence to support the notion that a lower blood pressure and less prevalence of hypertension are more common in women compared with the age-matched man. Apparently, these data will open a new view for novel therapeutic strategies against hypertension.

5 | CONCLUSION

Our finding not only revealed the cellular and physiological mechanism of this critical parasympathetic drive in healthy subjects, but also confirmed the important role of the female-specific myelinated Ah-type baroreceptor/baroreceptive neurons in neurocontrol of circulation and blood pressure regulation. The current data strongly supported our previous findings[6,8–10,12,14,16] and suggested a new potential pathway and cellular targets for pharmacological intervention for hypertension and related cardiovascular diseases.

CONFLICTS OF INTEREST

These authors declare no conflict of interest.

ORCID

Bai-Yan Li http://orcid.org/0000-0002-1853-0216

REFERENCES

1. Iscen S. Autonomic nervous system and hypertension. *Eur Rev Med Pharmacol Sci*. 2016;20:201.
2. Santa Cruz Chavez GC, Li BY, Glazebrook PA, et al. An afferent explanation for sexual dimorphism in the aortic baroreflex of rat. *Am J Physiol Heart Circ Physiol*. 2014;307:H910–H921.
3. Jin YH, Bailey TW, Li BY, et al. Purinergic and vanilloid receptor activation releases glutamate from separate cranial afferent terminals in nucleus tractus solitarius. *J Neurosci*. 2004;24:4709-4717.
4. He JL, Zhao M, Xia JJ, et al. FGF21 ameliorates the neurocontrol of blood pressure in the high fructose-drinking rats. *Sci Rep*. 2016;6:29582.
5. Kimmerly DS. A review of human neuroimaging investigations involved with central autonomic regulation of baroreflex-mediated cardiovascular control. *Auton Neurosci*. 2017;207:10-21.
6. Li BY, Qiao GF, Feng B, et al. Electrophysiological and neuroanatomical evidence of sexual dimorphism in aortic baroreceptor and vagal afferents in rat. *Am J Physiol Regul Integr Comp Physiol*. 2008;295:R1301–R1310.
7. Li BY, Schild JH. Patch clamp electrophysiology in nodose ganglia of adult rat. *J Neurosci Methods*. 2002;115:157-167.
8. Li BY, Schild JH. Electrophysiological and pharmacological validation of vagal afferent fiber type of neurons enzymatically isolated from rat nodose ganglia. *J Neurosci Methods*. 2007;164:75-85.
9. Liu Y, Wen X, Liu SZ, et al. KCa1.1-mediated frequency-dependent central and peripheral neuromodulation via Ah-type baroreceptor neurons located within nodose ganglia and nucleus of solitary tract of female rats. *Int J Cardiol*. 2015;185:84-87.
10. Liu Y, Zhou JY, Zhou YH, et al. Unique expression of angiotensin type-2 receptor in sex-specific distribution of myelinated ah-type baroreceptor neuron contributing to sex-dimorphic neurocontrol of circulation. *Hypertension*. 2016;67:783-791.
11. Lu XL, Xu WX, Yan ZY, et al. Subtype identification in acutely dissociated rat nodose ganglion neurons based on morphologic parameters. *Int J Biol Sci*. 2013;9:716-727.
12. Qiao GF, Li BY, Lu YJ, et al. 17Beta-estradiol restores excitability of a sexually dimorphic subset of myelinated vagal afferents in ovariectomized rats. *Am J Physiol Cell Physiol*. 2009;297:C654–C664.
13. Qiao GF, Li BY, Zhou YH, et al. Characterization of persistent TTX-R Na^+ currents in physiological concentration of sodium in rat visceral afferents. Int. *J Biol*. 2009;Sci 5:293-297.
14. Qiao GF, Qian Z, Sun HL, et al. Remodeling of hyperpolarization-activated current, Ih, in Ah-type visceral ganglion neurons following ovariectomy in adult rats. *PLoS One*. 2013;8:e71184.
15. Yan ZY, He JL, Wen X, et al. Variations in afferent conduction and axonal morphometrics of aortic depressive nerve imply wider baroreflex function of low-threshold and sex-specific myelinated Ah-type baroreceptor neurons in rats. *Int J Cardiol*. 2015;182:23-26.
16. Zhang YY, Yan ZY, Qu MY, et al. KCa1.1 is potential marker for distinguishing Ah-type baroreceptor neurons in NTS and contributes to sex-specific presynaptic neurotransmission in baroreflex afferent pathway. *Neurosci Lett*. 2015;604:1-6.
17. Anish TS, Shahulhameed S, Vijayakumar K, et al. Gender difference in blood pressure, blood sugar, and cholesterol in young adults with comparable routine physical exertion. *J Family Med Prim Care*. 2013;2:200-203.
18. Liu Y, Wu D, Qu MY, et al. Neuropeptide Y-mediated sex- and afferent-specific neurotransmissions contribute to sexual dimorphism of baroreflex afferent function. *Oncotarget*. 2016;7:66135-66148.
19. Voss A, Schroeder R, Fischer C, et al. Influence of age and gender on complexity measures for short term heart rate variability analysis in healthy subjects. *Conf Proc IEEE Eng Med Biol Soc*. 2013;2013:5574-5577.

20. Dutra SG, Pereira AP, Tezini GC, et al. Cardiac autonomic modulation is determined by gender and is independent of aerobic physical capacity in healthy subjects. *PLoS One*. 2013;8:e77092.
21. Abhishekh HA, Nisarga P, Kisan R, et al. Influence of age and gender on autonomic regulation of heart. *J Clin Monit Comput*. 2013;27:259-264.
22. Julius S, Randall OS, Esler MD, et al. Altered cardiac responsiveness and regulation in the normal cardiac output type of borderlind hlpertension. *Circ Res*. 1975;36:199-207.
23. Pothineni NV, Shirazi LF, Mehta JL. Gender Differences in Autonomic Control of the Cardiovascular System. *Curr Pharm Des*. 2016;22:3829-3834.
24. Koenig J, Thayer JF. Sex differences in healthy human heart rate variability: A meta-analysis. *Neurosci Biobehav Rev*. 2016;64:288-310.
25. Siddiqui AN, Siddiqui N, Khan RA, et al. Neuroprotective Role of Steroidal Sex Hormones: An Overview. *CNS Neurosci Ther*. 2016;22:342-350.
26. He JL, Li JN, Zuo CM, et al. Potentiation of 17beta-estradiol on neuroexcitability by HCN-mediated neuromodulation of fast-after-hyperpolarization and late-afterdepolarization in low-threshold and sex-specific myelinated Ah-type baroreceptor neurons via GPR30 in female rats. *Int J Cardiol*. 2015;182:174-178.
27. Wang LQ, Liu SZ, Wen X, et al. Ketamine-mediated afferent-specific presynaptic transmission blocks in low-threshold and sex-specific subpopulation of myelinated Ah-type baroreceptor neurons of rats. *Oncotarget*. 2015;6:44108-44122.
28. Niespodziany I, Andre VM, Leclere N, et al. Brivaracetam differentially affects voltage-gated sodium currents without impairing sustained repetitive firing in neurons. *CNS Neurosci Ther*. 2015;21:241-251.
29. Yu L, Zhang XY, Cao SL, et al. Na^+ -Ca^{2+} Exchanger, Leak K^+ Channel and Hyperpolarization-Activated Cyclic Nucleotide-Gated Channel Comediate the Histamine-Induced Excitation on Rat Inferior Vestibular Nucleus Neurons. *CNS Neurosci Ther*. 2016;22:184-193.
30. Ma C, LaMotte RH. Multiple sites for generation of ectopic spontaneous activity in neurons of the chronically compressed dorsal root ganglion. *J Neurosci*. 2007;27:14059-14068.
31. Jin YH, Bailey TW, Doyle MW, et al. Ketamine differentially blocks sensory afferent synaptic transmission in medial nucleus tractus solitarius (mNTS). *Anesthesiology*. 2003;98:121-132.
32. Qiao GF, Cheng ZF, Huo R, et al. GM1 ganglioside contributes to retain the neuronal conduction and neuronal excitability in visceral and baroreceptor afferents. *J Neurochem*. 2008;106:1637-1645.
33. Bailey TW, Jin YH, Doyle MW, et al. Vasopressin inhibits glutamate release via two distinct modes in the brainstem. *J Neurosci*. 2006;26:6131-6142.
34. Jones HC, Keep RF. Brain fluid calcium concentration and response to acute hypercalcaemia during development in the rat. *J Physiol*. 1988;402:579-593.
35. Doyle MW, Andresen MC. Reliability of monosynaptic sensory transmission in brain stem neurons in vitro. *J Neurophysiol*. 2001;85:2213-2223.
36. Lin M, Liu R, Gozal D, et al. Chronic intermittent hypoxia impairs baroreflex control of heart rate but enhances heart rate responses to vagal efferent stimulation in anesthetized mice. *Am J Physiol Heart Circ Physiol*. 2007;293:H997–H1006.
37. Li JN, Qian Z, Xu WX, et al. Gender differences in histamine-induced depolarization and inward currents in vagal ganglion neurons in rats. *Int J Biol Sci*. 2013;9:1079-1088.
38. Guo JM, Shu H, Wang L, et al. SIRT1-dependent AMPK pathway in the protection of estrogen against ischemic brain injury. *CNS Neurosci Ther*. 2017;23:360-369.
39. Lim DW, Kim JG, Lee Y, et al. Preventive effects of Eleutherococcus senticosus bark extract in OVX-induced osteoporosis in rats. *Molecules*. 2013;18:7998-8008.
40. Folkow B. Physiological aspects of primary hypertension. *Physiol Rev*. 1982;62:347-504.
41. Oparil S. The sympathetic nervous system in clinical and experimental hypertension. *Kidney Int*. 1986;30:437-452.
42. Mark AL. The sympathetic nervous system in hypertension: a potential long-term regulator of arterial pressure. *J Hypertens*. 1996;14:S159-S165.
43. Ramirez AJ, Bertinieri G, Belli L, et al. Reflex control of blood pressure and heart rate by arterial baroreceptors and by cardiopulmonary receptors in the unanaesthetized cat. *J Hypertens*. 1985;3:327-335.
44. Grassi G. Assessment of sympathetic cardiovascular drive in human hypertension: achievements and perspectives. *Hypertension*. 2009;54:690-697.
45. Julius S, Pascual AV, London R. Role of parasympathetic inhibition in the hyperkinetic type of borderline hypertension. *Circulation*. 1971;44:413-418.
46. Kim TH, Vemuganti R. Effect of sex and age interactions on functional outcome after stroke. *CNS Neurosci Ther*. 2015;21:327-336.
47. Reulecke S, Charleston-Villalobos S, Voss A, et al. Dynamics of the cardiovascular autonomic regulation during orthostatic challenge is more relaxed in women. *Biomed Tech (Berl)*. 2017;63:139-150.
48. Tan X, Jiao PL, Wang YK, et al. The phosphoinositide-3 kinase signaling is involved in neuroinflammation in hypertensive rats. *CNS Neurosci Ther*. 2017;23:350-359.

How to cite this article: Xu W-X, Yu J-L, Feng Y, et al. Spontaneous activities in baroreflex afferent pathway contribute dominant role in parasympathetic neurocontrol of blood pressure regulation. *CNS Neurosci Ther*. 2018;24:1219–1230. https://doi.org/10.1111/cns.13039